Contribution from the Department of Chemistry, Faculty of Science, University of Tokyo, Hongo, Tokyo and National Institute for Researches in Inorganic Materials, Tokyo

Far Infra-red Absorption Spectra of Layer Silicates

M. Ishii, T. Shimanouchi and M. Nakahira

Received September 23, 1967

Infra-red absorption spectra of layer silicates have been measured in the region from 1200 to 60 cm^{-1}. Normal coordinate treatments have been made of the ideal structure of dioctahedral and trioctahedral type micas. The observed absorption bands are assigned to the vibrations of Si_2O_5 layers and octahedral layers. The bands appearing in the region from 200 to 80 cm^{-1} are studied in detail and are assigned to the interlayer vibrations.

Introduction

Infra-red absorption spectra of layer silicates have been reported by several authors. Most of them have been measured in NaCl and KBr regions[1-8] and the spectra down to 300 cm^{-1} have been reported only for micas.[6] We have recently measured the infra-red spectra of various silicates down to 60 cm^{-1} and found many bands in the far infra-red region. The low temperature measurements have also been made. An interesting fact is that some of the bands become very sharp and split into two or more bands. The resulting low temperature spectra consist of many sharp bands and they seem to provide much information.

Normal coordinate treatments have been reported for the single layer of the Si_2O_5 lattice.[1,6,9] Since the results are not sufficient for the assignments of many bands measured in the present study, the treatments have been made for the single Si_2O_5 layer and also for the three dimensional layer lattice. The assignements of the bands have been given on the basis of the frequency calculations. The results are reported in the present paper.

Experimental Section

Specimens examined were supplied from various sources as follows: Muscovite: Single crystals from Ishikawa Mine, Japan; Phlogopite: Single crystals from Hoshi Mine, Korea; Brucite: Single crystals from Shinokuri, Fukuoka, Japan; Kaolinite: Powder crystals from Itaya Mine, Japan; Mg-Chlorite: Powder crystals from Wanibuchi Mine, Japan; Talc, Pyrophyllite and Hydrargillite (Synthesized): obtained from Dr. S. Suzuki of Government Chemical Industrial Research Institute.

The results of chemical analysis of talc, pyrophyllite, muscovite, phlogopite and Mg-chlorite used in this study are given in Table I.

Table I. Chemical Composition of Layer Silicates

	(I)	(II)	(III)	(IV)	(V)
SiO_2	68.66	40.92	57.11	39.27	29.07
Al_2O_3	25.82	38.81	3.77	17.52	21.82
Fe_2O_3	0.28	4.49	1.06	0.68	0.83
FeO		0.63		1.52	3.67
TiO_2	0.10	tr.	0.04		0.32
CaO	0.11	0.20	0.44		0.19
MgO	0.10	1.55	32.70	26.37	29.90
MnO		0.02			
K_2O	0.05	5.31		8.40	tr.
Na_2O	0.33	2.25		0.69	tr.
Li_2O		1.13			
F				0.63	
Ignition Loss	4.51	4.34	4.23	4.23	13.52

(I): Pyrophyllite; (II): Muscovite; (III): Talc; (IV): Phlogopite; (V): Mg-Chlorite.

Hitachi FIS-1 double beam vacuum spectrophotometer (500-60 cm^{-1}), Hitachi EPI-L double beam spectrophotometer (700-200 cm^{-1}) and Japan Spectroscopic 402G double beam spectrophotometer (1200-700 cm^{-1}) were used for the measurements of absorption spectra.

Infra-red and far infra-red absorption spectra of dioctahedral type layer silicate including kaolinite, pyrophyllite and muscovite are reproduced in Figure 2. The spectrum of hydrargillite, which has the octahedral layer structure, is given together. The measurements at liquid nitrogen temperature were also made by the use of the low temperature cells designed for these spectrophotometers[10] and the spectra are given in Figure 2. The dichroism measurements were made for the cleavage plane of muscovite. AgCl and polyethylene polarizers were used in the regions from 1200 to 650 cm^{-1} and from 700 to 60 cm^{-1}, respectively. The result is given in Figure 3. The spectra of trioctahedral type layer silicates including talc, phlogopite, biotite and lepidomelane are reproduced in Figure 4. In the

(1) B. D. Saksena, *Trans. Faraday Soc.*, *57*, 242 (1961).
(2) W. Vedder and R. S. McDonald, *J. Chem. Phys.*, *38*, 1583 (1963).
(3) B. I. Stepanov and A. M. Prima, *Optika Spektr.*, *5*, 15 (1958).
(4) V. Stubican and R. Roy, *Am. Mineral.*, *46*, 32 (1961).
(5) V. Stubican, *Zeit. Krist.*, *115*, 200 (1961).
(6) W. Vedder, *Am. Mineral.*, *49*, 736 (1964).
(7) M. Tsuboi, *Bull. Chem. Soc.* (Japan), *23*, 83 (1950).
(8) V. C. Farmer and J. D. Russell, *Spectrochim. Acta*, *20*, 1149 (1964).
(9) F. Mottosi, *J. Chem. Phys.*, *17*, 679 (1949).
(10) I. Harada and T. Shimanouchi, *J. Chem. Phys.*, *46*, 2707 (1967).

figure the spectrum of Mg-chlorite is also given. Chemical analysis shows that the composition of the sample used in the present work is

$$(Mg_{4.30}Fe_{0.30}^{2+}Fe_{0.06}^{3+}Al_{1.28})(Al_{1.20}Si_{2.80})O_{10}(OH)_8 .$$

The spectrum of brucite having the octahedral layer structure is also given together.

Normal Coordinate Treatments and Lattice Vibrations of Micas. The optically active lattice vibration frequencies were calculated according to the procedure based on the GF matrix method.[11,12]

The calculation was made for the following ideal models: (1) Si_2O_5 and $AlSi_3O_{10}$ monolayers, (2) 1M type dioctahedral and trioctahedral type micas. Numerical calculations were carried out by HITAC 5020 in the Computation Centre of University of Tokyo.

As shown in Figure 1, the structure of layer silicates consists of so-called "octahedral" and "tetrahedral" layers. In an octahedral layer the sites of octahedral

	Dioctahedral Type	Trioctahedral Type
Octahedral Layer	Hydrargillite Type $Al(OH)_3$	Brucite Type $Mg(OH)_2$
1:1 Type Structure	Kaolinite $Al_2(Si_2O_5)(OH)_4$	
2:1 Type Structure	Pyrophyllite $Al_2(Si_2O_5)_2(OH)_2$	Talc $Mg_3(Si_2O_5)_2(OH)_2$
Mica	Muscovite $KAl_2(AlSi_3O_{10})(OH)_2$	Phlogopite $KMg_3(AlSi_3O_{10})(OH)_2$ Biotite Lepidomelane

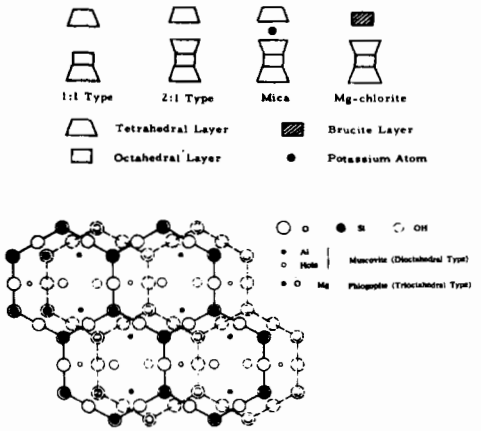

Figure 1. Structure of layer silicates.

coordination are occupied by either the tri- or the divalent positive ions. Generally, these ions are Al^{3+} or Mg^{2+}, and the basic structure of octahedral layer is of the hydrargillite-($Al(OH)_3$) or brucite-type ($Mg(OH)_2$). These are called dioctahedral type and trioctahedral type, respectively. The tetrahedral layer is a two dimensional Si_2O_5 network. In talc, pyrophyllite and micas the octahedral layer is placed between two tetrahedral layers (2:1 type structure), but in kaolinite it is placed between a Si_2O_5 layer and a OH layer (1:1 type structure) (Figure 1).

(11) T. Shimanouchi, M. Tsuboi and T. Miyazawa, *J. Chem. Phys.*, 35, 1597 (1961).
(12) I. Nakagawa and T. Shimanouchi, *Spectrochim. Acta*, 22, 1707 (1966).

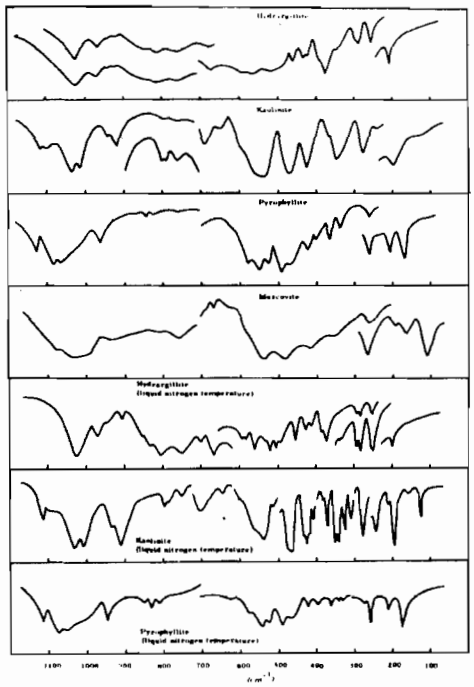

Figure 2. Far infra-red absorption spectra of layer silicates. (Dioctahedral type).

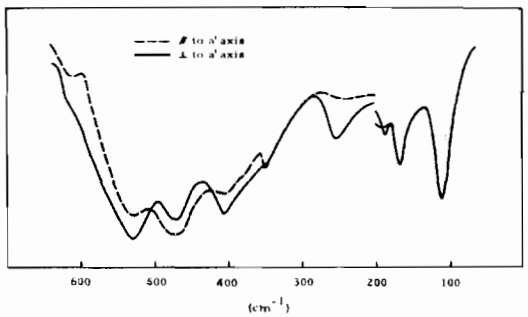

Figure 3. Infra-red dichroism of muscovite.

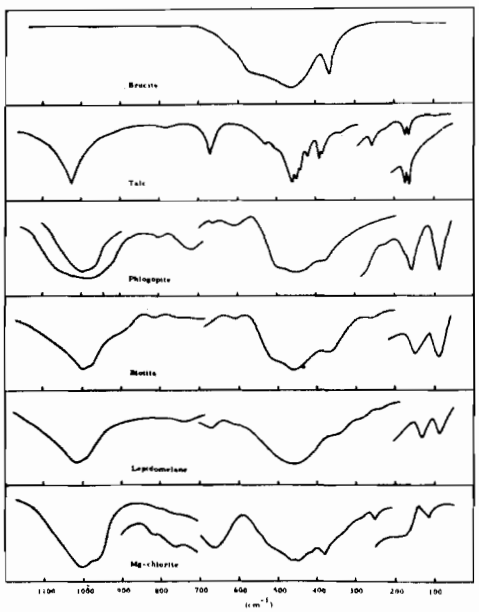

Figure 4. Far infra-red absorption spectra of layer silicates. (Trioctahedral type and Mg-chlorite).

In micas, parts of Si atoms of tetrahedral layer are substituted by Al atoms. The composite layer is negatively charged and cations (generally K^+ ions) are added simultaneously between the layers to keep the electrical neutrality. In muscovite and phlogopite, the substitution takes place up to a ratio 3Si-1Al.

The entire structure of the layer silicates is determined by the stacking arrangements of the composite layers, and the typical types are (1) one-layer monoclinic (1M type) structure, (2) two-layer monoclinic (2M type) structure, and (3) three-layer trigonal (3T type) structure.[13] Muscovite and phlogopite are crystallized in 1M or 2M type structure.

(I) *Normal coordinate treatments of Si_2O_5 and $AlSi_3O_{10}$ layers.* A two dimensional Si_2O_5 layer lattice has C_{6v} symmetry and a Bravais unit cell contains seven atoms (Si_2O_5). The factor group analysis shows that five vibrational modes are infra-red active (Table II).

Table II. Symmetry Species and Selection Rules

(1) S_2O_5 layer

C_{6v}	N	T	n	IR	R	C_{3v}	N	T	n	IR	R
A_1	3	1	2	a.	a.	A_1	4	1	3	a.	a.
A_2	0	0	0	ia.	ia.						
B_1	3	0	3	ia.	ia.	A_2	3	0	3	ia.	ia.
B_2	1	0	1	ia.	ia.						
E_1	4	1	3	a.	a.	E	7	1	6	a.	a.
E_2	3	0	3	ia.	a.						

(2) $AlSi_3O_{10}$ layer

C_s	N	T	n	IR	R
A′	26	2	24	a.	a.
A″	16	1	15	a.	a.

(3) Idealized 1M type mica

Dioctahedral type						Trioctahedral type					
C_{2h}^3	N	T	n	IR	R	C_{2h}^3	N	T	n	IR	R
A_g	16	0	16	ia.	a.	A_g	16	0	16	ia.	a.
B_g	14	0	14	ia.	a.	B_g	14	0	14	ia.	a.
A_u	15	1	14	a.	ia.	A_u	16	1	15	a.	ia.
B_u	21	2	19	a.	ia.	B_u	23	2	21	a.	ia.

IR: Infra-red; R: Raman; a: active; ia: inactive; N: Number of degrees of freedom; T: Number of overall translations of Bravais unit cell; n: Number of intramolecular vibrational modes.

The A_1 and E_1 modes have transition moments parallel and perpendicular to the c′ axis which is normal to the layer, respectively. The X-ray structure analysis shows that the SiO_4 tetrahedron group rotates about the non-bridged Si–O axis, half of them clockwise, the other half counterclockwise and the symmetry of the layer lattice is reduced to C_{3v}[14,15] (see Figure 5). As a result, a Bravais unit cell of this layer lattice contains the same number of atoms as the non-distorted one, having C_{6v} symmetry, and nine infra-red active vibrational modes are expected. The A_1 and E modes have transition moments parallel and perpendicular to the c′ axis,

(13) J. V. Smith and H. S. Yoder, *Min. Mag.*, *31*, 209 (1956).
(14) E. W. Radoslovich, *Acta Cryst.*, *13*, 919 (1960).
(15) H. Steinfink, *Am. Mineral.*, *47*, 886 (1962).

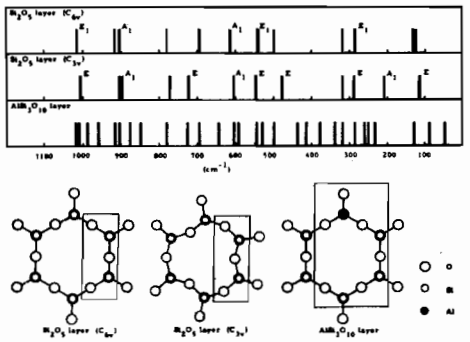

Figure 5. Calculated frequencies of Si_2O_5 layer and $AlSi_3O_{10}$ layer. Rectangles show Bravais unit cell.

respectively. In order to see the effects of Al substitution for Si in the tetrahedral layer, the calculation of the lattice vibrations of a $AlSi_3O_{10}$ layer was carried out in addition to the basic Si_2O_5 layer. If the Al substitution takes place regularly as indicated in Figure 5, the symmetry of the layer lattice is reduced to C_s, and thirty-nine infrared active vibrational modes are expected.

The potential function used in the calculation of F matrix is of the Urey-Bradley type and expressed as

$$\begin{aligned} V = {} & (1/2)\sum_{ij} K_{ij}(\Delta r_{ij})^2 + (1/2)\sum_{ijk} H_{ijk}[(r_{ij}r_{jk})^{1/2}\Delta\varphi_{ijk}]^2 \\ & + (1/2)\sum_{ik} F_{ik}(\Delta q_{ik})^2 + \sum \varkappa_h g_h(\Delta r_{ij}, \Delta\varphi_{ijk}) \\ & + (1/2)\sum_{ij} Y_{ij}(\Delta\tau_{ij})^2 \end{aligned} \qquad (1)$$

where r is the bond length, φ the bond angle, q the non-bonded atom distance and τ the angle of internal rotation. K, H, F and Y are the bond stretching, angle bending, repulsive and torsional force constants, respectively, $\varkappa_h$ is the internal tension and g_h is a function derived from the redundancy condition.[16] The structural parameters used in this calculation are listed in Table IV. At first the force constants were transferred from those of methylpolysiloxane determined by the normal vibration calculations.[17] Since the results gave slightly higher frequencies for the Si–O stretching vibration than the observed value,* 1019 cm^{-1} of talc, the value of K(Si–O) was adjusted and was given 3.508 md/Å. The recalculation gives the results shown in Figure 5. Force constants used are given in Table III. In the model of the distorted Si_2O_5 layer, the magnitude of rotation about non-bridged Si–O axis was assumed to be 12°. In these calculations, it was assumed that the force constants were not affected by the Al substitution for Si in the tetrahedral layer.

(II) *Vibrational modes of Si_2O_5 and $AlSi_3O_{10}$ layers.* The cleavage plane of micas is perpendicular to the c′ axis, so that the E_1 modes of Si_2O_5 layer lattice are expected to show strong absorptions in the spectra of the sheet of micas. Calculated frequencies of three E_1

(16) T. Shimanouchi, *Pure and Applied Chemistry*, *7*, 131 (1963).
(17) M. Ishii and T. Shimanouchi, unpublished.
(*) As for the assignment of this band, see discussions given in references (2) and (18).
(18) V. C. Farmer and J. D. Russel, *Spectrochim. Acta*, *22*, 389 (1966).

Table III. Force Constants

Si_2O_5 layer			
$K(Si-O)_{bridged.}$	3.508	F(O–Si–O)	0.074
$K(Si-O)_{non\text{-}bridged.}$	3.508	F(Si–O–Si)	0.045
H(OSiO)	0.389	$\varkappa$(Si)	0.107
H(SiOSi)	0.150	Y(Si–O)	0.020
Dioctahedral Type Mica		Trioctahedral Type Mica	
K(O–H)	7.350	K(O–H)	7.640
H(AlOH)	0.090	H(MgOH)	0.065
F(Al–O–H)	0.050	F(Mg–O–H)	0.050
K(Al–O)	2.100	K(Mg–O)	0.320
K(Al–OH)	2.100	K(Mg–OH)	0.320
H(AlOSi)	0.060	H(MgOSi)	0.100
F(Al–O–Si)	0.050	F(Mg–O–Si)	0.050
H(OAlO)	0.200	H(OMgO)	0.040
F(O–Al–O)	0.050	F(O–Mg–O)	0.050
H(AlOAl)	0.100	H(MgOMg)	0.050
F(Al–O–Al)	0.050	F(Mg–O–Mg)	0.050
f(KO)	0.060	f(KO)	0.050
K, H, F, f - - - md/Å		$\varkappa$, Y - - - md · Å	

Table IV. Structural parameters used in the calculation

r(Si–O)	1.60 Å	r(Mg–O)	2.06 Å
r(Al–O)	2.06 Å	r(Mg–OH)	2.06 Å
r(Al–OH)	2.06 Å	q(KO)	3.09 Å

modes are 1015, 543 and 285 cm^{-1}. As shown in Figure 6, the mode of 1015 cm^{-1} is the SiOSi antisymmetric stretching type, and that of 543 cm^{-1} is a coupling mode between the SiOSi symmetric stretching and the SiOSi bending motions. The mode of 285 cm^{-1} is interpreted as the motion of non-bridged oxygen atoms against bridged ones. Calculated frequencies of the two A_1 modes are 902 and 613 cm^{-1}. The former is a motion of silicon atoms against oxygen atoms and the latter is a totally symmetric stretching mode of each tetrahedron.

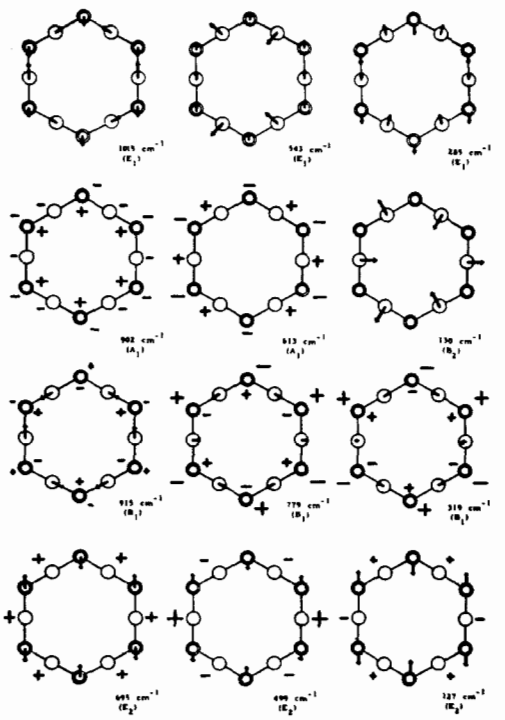

Figure 6. Vibrational modes of Si_2O_5 layer lattice. The large circle denotes the oxygen atom and the small circle the silicon atom. + and – outside of the hexagon denote the perpendicular displacements of the oxygen atom and those inside of the hexagon denote the displacement of the silicon atom.

For the distorted Si_2O_5 layer lattice, the number of E modes, which have a transition moment parallel to the c′ axis, is six. In contrast to the non-distorted case, three vibrations at 722, 476 and 113 cm^{-1} become infra-red active and are expected to show strong absorption bands. Calculated frequencies of three A_1 modes are 895, 603 and 209 cm^{-1}. When the Al substitution takes place, the splitting or broadening of absorption bands is expected as shown in Figure 5.

(III) *1M type dioctahedral and trioctahedral type micas.* In order to investigate vibrations of octahedral layers and potassium atoms between the silicate layers, the optically active lattice vibrations of idealized dioctahedral and trioctahedral type micas were calculated. In this calculation, it is assumed that the Si_2O_5 layer is not distorted and the Al substitution does not take place. The stacking arrangement of the layers is assumed to be of the 1M type. Accordingly, it is assumed that the crystal structure is monoclinic and the space group is C_{2h}^3 (C2/m). The Bravais unit cell contains twenty-one atoms for the dioctahedral type mica and twenty-two atoms for the trioctahedral type mica. The factor group analysis shows that the vibrational modes of dioctahedral type mica are $16A_g+14A_u+14B_g+19B_u$ and those of trioctahedral type mica are $16A_g+15A_u+14B_g+21B_u$. Of these the A_u and B_u modes are infra-red active. The structural parameters used in this calculation are listed in Table IV. The potential function is expressed as

$$V = V_{intralayer} + V_{interlayer} \qquad (2)$$

where $V_{intralayer}$ is the intralayer potential of $Al_2(Si_2O_5)_2(OH)_2$ or $Mg_3(Si_2O_5)_2(OH)_2$ layer and $V_{interlayer}$ is the interaction potential between the positive ions and those layers. For $V_{intralayer}$ the Urey-Bradley force field given above was used. The interlayer interaction potential is assumed to arise from the interaction between the positive ion (K^+) and the neighbouring twelve oxygen atoms.

$$V_{interlayer} = (1/2)\sum_i f^i(KO)[\Delta q^i(KO)]^2 \qquad (2)$$

where q(KO) is the distance between a K^+ ion and an oxygen atom and the f(KO) is the corresponding force constant.

In this calculation, the force constants of the Si_2O_5 layer were assumed to be same as described above. For the octahedral layer, the force constants were estimated from those determined by the normal coordinate treatments of complex salts[19] and organometallic compounds.[20] The interlayer interaction force constant f(KO) was adjusted to obtain the best agreement between the observed and the calculated frequencies of the vibrations of potassium atoms between the silicate

(19) I. Nakagawa and T. Shimanouchi, *Spectrochim. Acta*, *20*, 429 (1964).
(20) T. Onishi and T. Shimanouchi, *Spectrochim. Acta*, *20*, 325 (1964).

layers discussed below. Observed and calculated frequencies are shown in Figure 7.

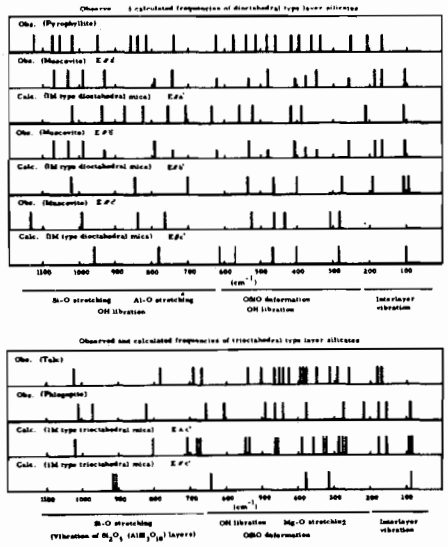

Figure 7. Observed and calculated frequencies of di- and trioctahedral type layer silicates.

Vbirations of Dioctahedral and Trioctahedral Type Layer Silicates. As shown in Figure 2, the vibrations of tetrahedral layers and those of octahedral layers are overlapped in the region from 1200 to 150 cm^{-1} for the spectra of dioctahedral type layer silicates. On the basis of the result of the calculations given above, the assignments of the absorption bands of pyrophyllite and muscovite in this region have been made. In the region from 1200 to 650 cm^{-1}, Si–O stretching, Al–O stretching and OH libration frequencies, and, in the region from 650 to 250 cm^{-1}, OSiO deformation and OH libration frequencies are expected.

As for the OH libration frequencies, Vedder *et al.*[2] assigned them to the 925 and 405 cm^{-1} bands of muscovite, since they shift to lower frequencies on deuteration. These two bands show opposite dichroism and the 405 cm^{-1} band shows the same behaviour as the OH stretching band at 3642 cm^{-1}. Since muscovite has the 2M type structure, the correspondance between the observed and the calculated frequencies is not straightforward. By taking into account the stacking arrangement of the layer and the direction of the OH ions, 925 and 405 cm^{-1} bands are assigned to the bands belonging to A_u and B_u species of the 1M type model, respectively. In the region below 250 cm^{-1} absorption bands due to the interlayer vibrations are expected and they are discussed below separately.

The spectra at liquid nitrogen temperature are reproduced in Figure 2. For kaolinite the absorption bands below 500 cm^{-1} become sharp and some of them show splittings. For hydrargillite the sharpenings and the splittings of the bands in the same region are also observed. These facts suggest that these bands are associated with the vibrations of OH ions which interact with each other by the inter- or intralayer hydrogen bonding type associations. For pyrophyllite most of the bands are pretty sharp at room temperature and do not show sharpening and splitting at low temperature. In fact, in the structure of pyrophyllite no hydrogen bonding is involved.

In contrast to pyrophyllite, the absorption bands of muscovite are very broad probably due to the irregularity of the Si_2O_5 tetrahedral layers caused by the substitution of aluminum atoms. They does not show sharpening and splitting even at low temperature.

The dichroism observed for muscovite in the cleavage plane is reproduced in Figure 3 in the region from 700 to 60 cm^{-1}. All the observed bands except those at 168 and 108 cm^{-1} show distinct dichroism. In the spectra of the sheet tilted by 45° to the incident light and those of powder, other weak shoulder bands were observed. These bands are assigned to the vibrational modes with transition moments perpendicular to the ab plane (the cleavage plane).

As for the trioctahedral type layer silicates, the structure of the octahedral layer is of the brucite type. As shown in Figure 4, brucite has no band in the region from 1200 to 700 cm^{-1} in contrast to the spectrum of hydrargillite, which has strong bands associated with the Al–O bond in this region. The Mg–O bond of brucite is weaker than the Al–O bond of hydrargillite as revealed by the X-ray diffraction measurement[21,22] and the bands associated with the Mg–O bonds become probably lower than 700 cm^{-1}.

For the normal coordinate treatments we used the Mg–O stretching force constant which was transferred from those of $[Mg(H_2O)_6]^{2+}$ and which was considerably smaller than that of the Al–O bond. As shown in Figure 7, the calculated Mg–O stretching frequencies are lower than 700 cm^{-1}. This result is consistent with above assignments of the spectrum of brucite.

The spectra of the trioctahedral type layer silicates have some bands in the region from 1200 to 700 cm^{-1} as shown in Figure 4. These bands are assigned to the vibrations of the Si_2O_5 or $AlSi_3O_{10}$ layers. Talc has one strong and isolated band at 1019 cm^{-1}, in agreement with the calculation as shown in Figure 7, and is assigned to the Si–O stretching mode. This band of talc does not show any splitting even at liquid nitrogen temperature, showing that the existence of the octahedral layer does not affect the vibrations of the Si_2O_5 layer in this region. In the region from 1200 to 700 cm^{-1}, phlogopite has a few broad absorption bands in agreement with the calculation for the $AlSi_3O_{10}$ layer shown in Figure 5. Biotite and lepidomelane, having the $AlSi_3O_{10}$ layer, have similar broad bands in this region.

In the region from 700 to 250 cm^{-1} the trioctahedral type layer silicates have many bands assigned to the Mg–O stretching, OSiO deformation and OH libration modes. Talc has many sharp bands in this region. Phlogopite, having the $AlSi_3O_{10}$ structure, has broad bands. The spectrum of biotite in this region is similar to that of phlogopite. The spectrum of lepidomelane in this region are broader than those of phlogopite and biotite, showing the irregularity of atomic arrangements caused by the incleasing Fe substitutions.

(21) H. D. Megaw, *Zeit. Krist.*, *87*, 185 (1934).
(22) H. E. Petch and H. D. Megaw, *J. Opt. Soc. Am.*, *44*, 744 (1954).

The absorption bands of phlogopite for the cleavage plane do not show dichroism as expected from the structure.

Interlayer Vibrations. In the region below 250 cm^{-1} most of the silicates have a few bands with considerable intensities. As shown in Figures 2 and 4 pyrophyllite, talc and muscovite have two bands in the region from 250 to 130 cm^{-1} and phlogopite has one band with a shoulder in this region. The results of calculation show that the trioctahedral type silicate, phlogopite, has two bands at 178 cm^{-1} (A_u) and 159 cm^{-1} (B_u) and the dioctahedral type silicate, muscovite, has two bands at 211 cm^{-1} (A_u) and 190 cm^{-1} (B_u). The vibrational modes of these bands are given in Figure 9, showing that they are the interlayer vibrations. The observed two

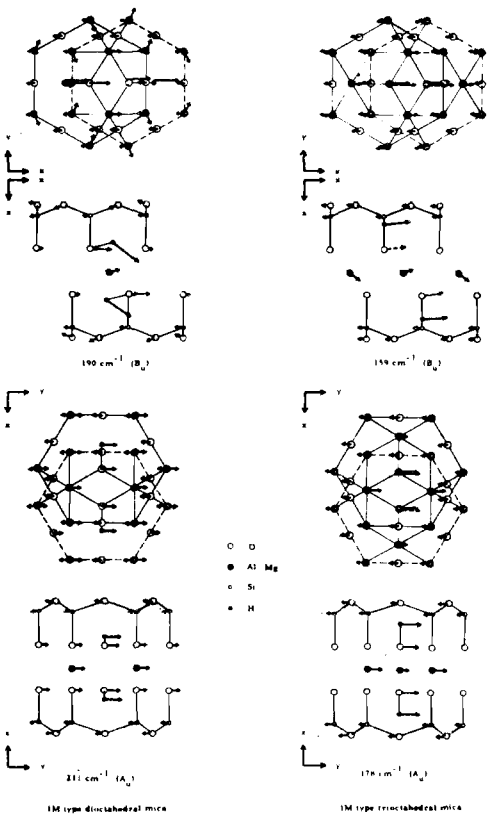

Figure 9. Modes of interlayer vibrations.

bands are assigned to the two interlayer vibrations, since the frequencies are close to the calculated. Furthermore the bands in this region shift to lower frequencies for lepidomelane, in which the magnesium atoms are partially substituted by the iron atoms in the octahedral layer supporting the above assignments.

In the region below 130 cm^{-1} the spectrum of muscovite has one band at 108 cm^{-1} in contrast to the spectra of pyrophyllite and kaolinite, which have no band in this region. Phlogopite, biotite and lepidomelane have also one band at about 90 cm^{-1} in contrast to that of talc, which have again no band in this region.

The result of calculation show that the 1M type model has four infra-red active vibrational modes in this region. As shown in Figure 8, those modes correspond to the three translational modes of the potassium atom and the torsional mode of the Si_2O_5 layer lattice. Since the band associated with the last mode are weak and one of those translational modes does not appear in the spectrum of the cleavage plane, the two K^+ translational modes with almost the same frequencies are expected to appear in the lower frequency region. The observed 108 cm^{-1} band of muscovite and the 90 cm^{-1} band of phlogopite, biotite and lepidomelane are assigned to this mode.

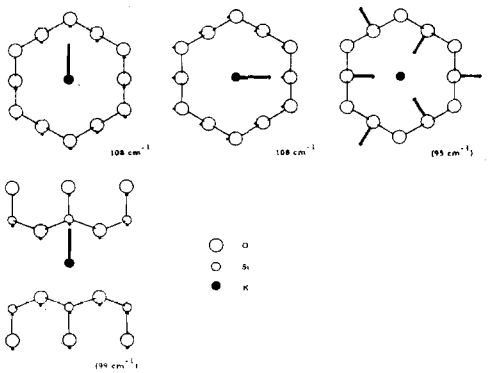

Figure 8. Modes of the vibration of potassium atom between the silicate layers of muscovite. ( )-- Calculated frequency.

We adjusted the force constant f(KO) so that the K^+ translational modes have the frequency of 108 cm^{-1} for muscovite and 90 cm^{-1} for phlogopite and other trioctahedral type micas. The obtained force constants are 0.06 md/Å for muscovite and 0.05 md/Å for phlogopite. X-ray diffraction study show[14,15] that the $AlSi_3O_{10}$ layer lattices of muscovite and phlogopite are distorted and the distances between the twelve oxygen atoms and the potassium atoms are not equal. In muscovite the distances between the potassium atom and the nearest six oxygen atoms are 2.81 Å and that between the potassium atom and the second nearest six oxygen atoms are 3.39 Å. In phlogopite these distances are 2.94 Å and 3.45 Å, respectively. The fact that the K^+--O distances of phlogopite is larger is in consistent with the present results that the K^+--O stretching force constant of phlogopite is smaller than that of muscovite. The values of f(KO) obtained are of the same magnitude as those obtained in complex salts.[12]

Mg-chlorite. The spectrum is reproduced in Figure 4. In Mg-chlorite a brucite layer is placed between the two silicate layers. The observed spectrum in the region from 1200 to 700 cm^{-1} supports the chemical composition given before in which silicon atoms of the silicate layer are partially substituted by the aluminum atoms. The spectrum has a sharp band at 383 cm^{-1}. The frequency is the same as that of a strong band in brucite. This band may be a key band for the brucite-type structure.

Acknowledgments. The authors wish to express their sincere thanks to Dr. S. Suzuki of Government Chemical Industrial Research Institute for his generous offer of the samples investigated in this report. Their thanks are also due to Dr. I. Nakagawa of the University of Tokyo for helpful discussion.